EVM of a cascaded MZM A-RoF transmitter for high order QAM

Jon Elipe Fonollosa and Miquel Sánchez Queralt
Universitat Politècnica de Catalunya (UPC)

Tutorized by María Santos (*UPC*)
(Dated: June 4, 2023)

Abstract: The paper deals with the transmission of modulated RoF data signals for 16-QAM and 64-QAM with a cascaded MZM transmitter. Performance according to EVM is later studied according to V_{B2} parameter of the transmitter and optimal transmission conditions are found. Also a brief test for increased frequency f_{RF} of the transmitter is carried out for QPSK modulation.

Usage: Secondary publications complementary to this one are [1] and [2].

Keywords: Radio-over-fiber, fixed-radio, signal modulation, Error Vector Magnitude

I. INTRODUCTION

This article is set as a continuation to *Monte Carlo BER Simulation of Radio Over Fiber Communication Links* [1] and an extension of *Optical Transmitters with Radio Frequency Extension for Analog Radio Over Fiber Fronthaul* [2]. Taking the cascaded MZM A-RoF transmitter designed in the [2] as the keystone of our investigation, and the computer simulation raised in [1] as a base, our research is centered on the performance of the transmitter for higher order Quadrature Amplitude Modulation (QAM) according to EVM parameter and the study of data transmission for frequencies greater than 10 GHz.

A. PON architecture diagram

The designed MZM A-RoF transmitter is intended to be used in a converged fiber, splitter-based PON environment. Passive Optical Network (PON) is a telecommunications network architecture that uses fiber-optic cables and passive components to provide high-speed data, voice, and video services to multiple end-users. In a PON, the bandwidth is shared among the subscribers, meaning that the available capacity is divided among the connected users. Further on, a splitter-based Passive Optical Network (PON) utilizes optical splitters to distribute the optical signals from the central office to multiple subscribers. Converged fiber means various service types are multiplexed or transmitted simultaneously over the same optical network.

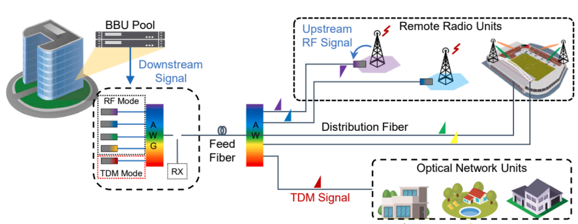

Figure 1. PON architecture diagram. Source: [3]

B. Cascaded MZM A-RoF transmitter

In order to explain the designed transmitter, the Mach-Zehnder Modulator (MZM) should be first introduced: an input optical signal is split into two branches in which the electrical driving signal changes the optical phase in a linear way. For the push-pull configuration the same signal with different signs is fed to each branch $V_1 = -V_2$ so $V = |V_1| = |V_2|$ is better defined in such a way that $V_i(t) = V_{B_i} + v_{RF_i}(t)$ is the drivng signal of the modulator. Quadrature Point (QP) is a relevant work point on MZM transfer function located midpoint between maximum and null power points. QP is special since it presents a linear relation between the driving signal and the optical power for small signal cases. It is also interesting to introduce Null Point (NP), since it is used in the designed transmitter: it is the work point located at the minimum of the power transfer function.

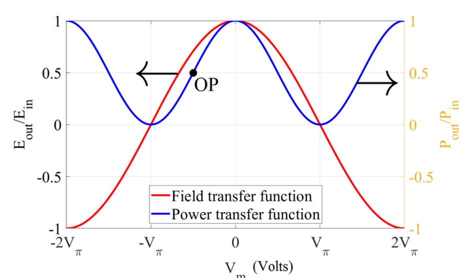

Figure 2. Plot of field (red) and power (blue) transfer functions of a Mach-Zehnder modulator working in push-pull configuration. Source: [4]

1. *Measurement and characterization of the transfer function of a MZM*

A measure of the transfer function of a MZM was done in the laboratory. The setup consisted on a generator and a laser source with its temperature controller. The fiber was attached to the polarization controller and to the power-meter and was set in a position to obtain an acceptable level of power. The MZM was connected and several values of V were used to characterize the response of the Mach-Zehnder Modulator.

In the following figure, the data about the function transfer measured are presented:

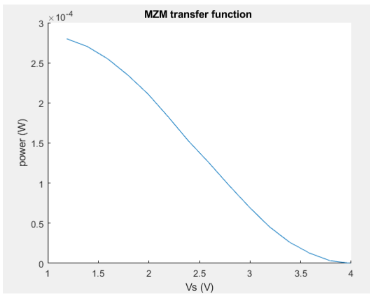

Figure 3. Measured power transfer function for single MZM

Further on, as seen in Figure 4, the transmitter is first composed of MZM1 driven by a pure tone signal with frequency f_{RF} and biased at the Null-Point (NP) with the purpose of outputting two optical carrier frequencies equispaced from zero and distanced between them by $2f_{RF}$. Next to it, MZM2 is found, which recieves the data vector at frequency f_{IF}, and its bias (V_{B_2}) is set so that a Double-Sided Band plus Carrier (DSB-C) modulation of the data is ensured over the carrier frequencies from the first MZM.

Now consider $m_1 = \pi V_{RF_1}/V_{\pi 1}$, with $V_{\pi 1}$ the half-wave voltage of MZM1 and V_{RF_1} the peak amplitude of the driving signal. For the small signal case, $m_1 << 1$, the output of the presented transmitter is a radio data signal at frequency $f_{RX} = 2f_{RF} \pm f_{IF}$ received at the photodetector output. On the other side, for a value equal to the first zero of the first order Bessel function $J_1(x)$, this is $m_1 \approx 3.8317$, first-order sidebands are minimized and higher order ones are generated, so that radio data signal is found instead at $f_{RX} = 6f_{RF} \pm f_{IF}$. However, our research is carried out for small driving signal case in MZM1.

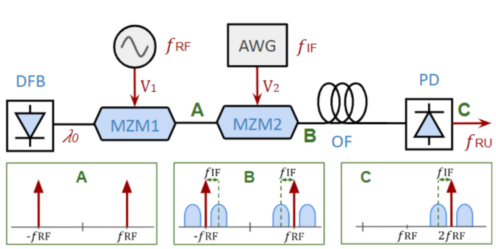

Figure 4. Schematic of the proposed optical transmitter with two cascaded PP-MZM Source: [2]

II. LABORATORY SETUP

In order to replicate the scheme of the transmitter, two cascaded MZM with $V_\pi = 3$ V and Extinction Rate $ER = 45$ dBm have been set up. The driving signal for each MZM is a combination of signals from a *Rhode & Schwartz* NGE100 · Power Supply Series continuous voltage source, which sets MZM1 to NP with $V_{B1} = 4.00$ V and also outputs V_{B2}, and a *Rhode & Schwartz* SMA 100B · Signal Generator in order to set $f_{RF} = 2.5$ GHz carrier frequency in MZM1 and a *Rhode & Schwartz* SMW 200A · Vector Signal Generator, which emits the data signal with frequency $f_{IF} = 1$ GHz inputed at MZM2 with the objective to be detected at the other end of the fiber. Using a *Rhode & Schwartz* FSW · Signal & Spectrum Analyzer · 2Hz-43.5GHz spectrometer, the data signal sidebands and carrier peak can be observed at their respective frequencies: $f_{RX} = 4$ GHz, $f_{RX} = 6$ GHz and $f_{RF} = 5$ GHz respectively.

A laser source is connected to the Vector Signal Generator in order to convert electric radiofrequency signal into optic signal immediately sent along the optical fiber. Later on a polarization controller is set so the polarization of the EM wave is best adapted to the conditions of the fiber. Finally both cascaded MZM are connected to the setup and their output is divided. One branch goes to an optical power-meter where a fixed $P_{rx} = -23$ dBm is expected. This value is chosen as a compensation of its range of voltages that can be achieved with this constant power and its performance. The other branch is directed to the spectrum analyzer which directly calculates the EVM value with the respective type of modulation that has been produced in the generator. A map of the constellation and the spectrum of the signal can also be seen in the Spectrum Analyzer.

III. EVM STUDY FOR 16QAM, 64QAM

BER is the figure of most merit over other performance metrics for advanced modulation, it requires a known pattern and is simply defined as the number of bit errors for unit time. On the other hand, EVM is a good performance measure in digital wireless communication systems for the quality of vector modulated signals and is a better and more appropriate way at high signal-noise ratio, where a large number of symbols would otherwise be required for accurate counting of errors with BER. The EVM metric is standard in wireless and wireline communications. However, its connection to BER and OSNR is not well established in optical communications.

QAM modulation of the M order encode a data signal in amplitude and phase of the optical electric field, this can be represented in the complex plane and results as a *constellation* of points, the square grid that can be found on Figure 5 (a) for 16-QAM. The received signal is not so precise, as it can be seen in the adjacent plot since white gaussian noise (WGN) is applied to the data signal along the fiber. WGN has two main sources: first thermal noise, due to electron agitation in the conductor, and second shot noise, due to Poisson distribution on the arrival time of the photons to the photodetector (it depends on the strength of the signal). The variances of both signals are the following, being BW the bandwidth of the data signal:

$$\sigma_{th} = \sqrt{\frac{2k_B T}{R_L} BW} \qquad \sigma_{sh} = \sqrt{q\frac{e}{hf_0}|x_t|^2 BW} \tag{1}$$

Another source of signal distortion is dispersion along the optical fiber, since photons spread out of the optical path as they travel, but its effect is negligible compared to WGN sources, so it is neglected in most studies.

Finally Error Vector Magnitude (EVM) is classically defined as follows for a number of I randomly transmitted data:

$$EVM_m = \frac{\sigma_{err}}{|E_{t,m}|} \qquad \sigma_{err}^2 = \frac{1}{I}\sum_{i=1}^{I}|E_{r,i} - E_{t,i}|^2 \tag{2}$$

where vector E_r represents the received signal, distanced a certain error vector E_{err} from the ideal transmitted E_t vector, according to Figure 5 (a). Despite this first definition, following EVM_a will be used, which is normalized by the average power $|E_{t,a}|^2$ of all M symbol vectors within a constellation.

$$EVM_a = kEVM_m \quad k^2 = \frac{|E_{t,m}|^2}{|E_{t,a}|^2} \quad |E_{t,a}|^2 = \frac{1}{M}\sum_{i=1}^{M}|E_{t,i}|^2 \tag{3}$$

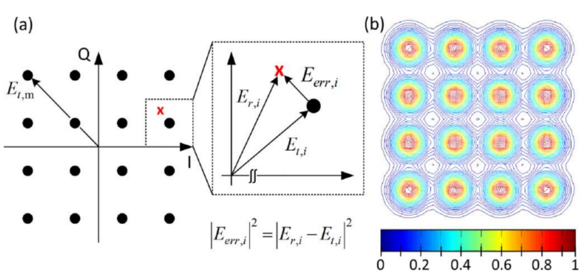

Figure 5. a) 16-QAM constellation vectors and b) WGN plot. Source: [5]

A. General behaviour of EVM and lab measurements

A computer simulation has been implemented using MATLAB in order to obtain the values of EVM as a function of V_B from MZM2 for higher order modulations 16-QAM and 64-QAM. This results are compared with real data obtained in laboratory. For all EVM results, including simulation and real data, recieved power is fixed at $P_{rx} = -23$ dBm.

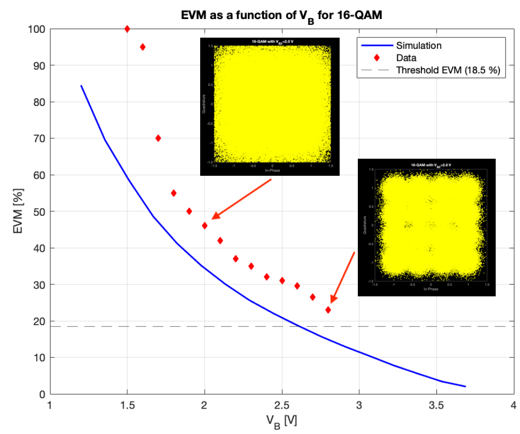

Figure 6. EVM as a function of V_B for 16-QAM

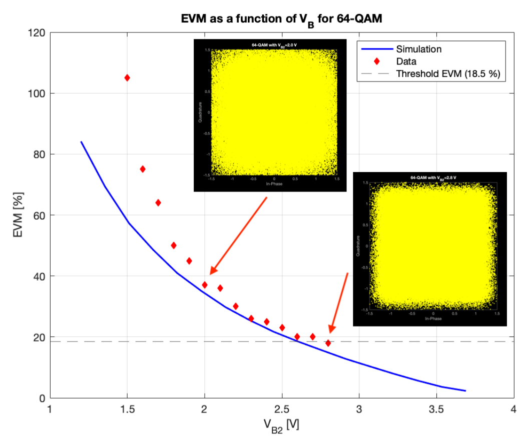

Figure 7. EVM as a function of V_B for 64-QAM

In figures 6 and 7, the respective plots (in 16-QAM mod. and in 64-QAM mod.) of EVM variation respect to V_B giving constant power obtained in the laboratory. They represent the values obtained experimenally respect to the simulated ones. Although the normalized simulation results have been adapted to the real $V_\pi = 3$ V value for MZM1 and a 0.75 V offset, certain systematic error is still present, being more noticeable in 16-QAM modulation. As is clearly seen in both plots the achievable range of constant power has a limit that can not be overpassed physically (the system cannot give the same power for higher values of V_B), but it can be computed without problem. If we observe the numerical values of the EVM in the diferent modulation types, we can notice that for the same voltage and increasing the modulation order (Bits per Symbol) the EVM dicreases, since although it takes a smaller error for a point on a constellation to pass to another, there are also more points in the constellation which supercompensates this effect. Nevertheless we cannot compare directly EVM values from one modulation order to a diferent one, since the acceptable EVM depends on the modulation order.

B. Minimum EVM and optimal OCSR relation

When studying the end of the EVM curve closely, it's possible to find a trend change in the monotonous decrease when approaching V_B values close to saturation (this is, $b_2 = 1$ for $V_{B2} = b_2 V_\pi + V_{offset}$). If the simulation is ran again choosing b_2 appropriately so that V_B values are in an interval of 3.6-3.74 V, the global minimum of EVM as a function of V_B can be found.

Optical carrier-to-sideband ratio (OCSR) is defined as a quocient of the power of carrier signal (already introduced in Figure 4 in the frequency domain) and power of the sideband signals, the one that contains the information to be transmitted along the fiber. Values of OCSR bigger than one mean power of the carrier signal is greater than that of the data signal. The optimal case is that of OCSR=1, for which the added power of both sideband signals equals the central carrier one.

As it can be observed in following Figures 8 and 9, optimal OCSR=1 is reached for value $V_{B2} = 3.68$ V for both 16-QAM and 64-QAM. It's important to notice for the same value of V_{B2} the minimum of EVM is found, meaning the optimal OCSR ensures the least error for the transmitted data signal.

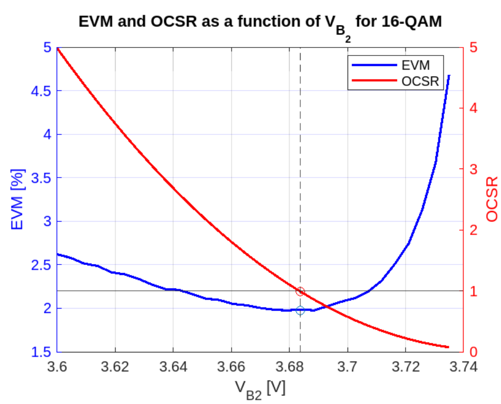

Figure 8. EVM and OCSR as a function of V_B for 16-QAM

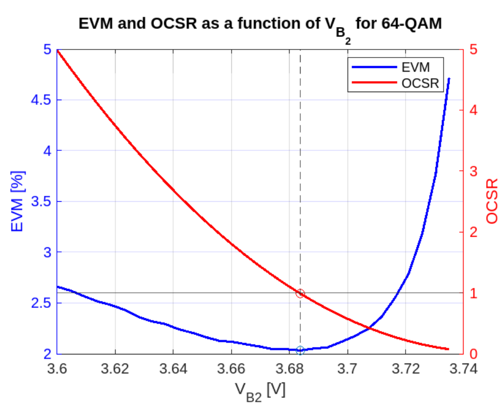

Figure 9. EVM and OCSR as a function of V_B for 64-QAM

IV. INCREASE OF DETECTION FREQUENCY

A novelty compared to previous research has been the use of a 20 GHz photodetector at the end of the optic fiber, compared to previous 10 GHz for QPSK/4-QAM modulation. A backdraw is that this dispositive has no signal amplifier, but has allowed the increment of the frequency of MZM1 pure tone input to $f_{RF} = 8$ GHz, and the data signal frequency to $f_{IF} = 1$ GHz. According to theory, the signal should be detected at $f_{RX} = 2f_{RF} \pm f_{IF}$, meaning $f_{RX} = 15$ GHz and $f_{RX} = 17$ GHz. The detected spectrum in frequency domain is shown in the following figure, verifying the expected results: the main spike appearing at the center corresponds to the $2f_{RF} = 16$ GHz periodic neighbour of the carrier frequency, and received data signal spikes are equispaced at ± 1 GHz each. Shown spectrum has been obtained setting $V_{B2} = 2.2$ V, for which received signal scatterplot looks as included in the figure.

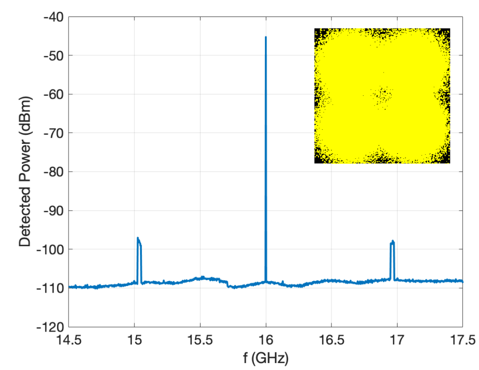

Figure 10. Detected spectrum in frequency domain

V. CONCLUSION

We have been able to extend simulations and real data to other modularion orders (16-QAM and 64-QAM) obtaining a close result between the simulated and measured data. Both have been satisfactory results even their limitations in the process, physical ones in the laboratory results, and memory ones in the simulated ones. The simulations used in this project can also be easily modified in order to test other types of modulation so better error conditions and performances can be researched easily.

Further research could be done on relating different error parameters: EVM, BER and OSCR obtained for the simulation. Also higher order QAM modulations could be studied for the increased f_{RX} case with improved laboratory equipment.

REFERENCES

[1] Sara Cabanas and Carla Macías. "Monte Carlo BER Simulation of Radio Over Fiber Communication Links". In: (2022).

[2] Sara Vega, María Santos, and Josep Prat. "Optical Transmitters with Radio Frequency Extension for Analog Radio Over Fiber Fronthaul". In: (2023).

[3] Caio L.M.P. Plazas et al. "Colorless WDM-PON fronthaul topology for beyond 5G C-RAN architectures". In: *Optical Fiber Technology* 76 (2023), p. 103244. ISSN: 1068-5200. DOI: `https://doi.org/10.1016/j.yofte.2023.103244`. URL: `https://www.sciencedirect.com/science/article/pii/S1068520023000238`.

[4] Debanuj Chatterjee. "A theoretical investigation of fiber phase sensitive amplifiers for applications". PhD thesis. Jan. 2021.

[5] René Schmogrow et al. "Error Vector Magnitude as a Performance Measure for Advanced Modulation Formats". In: *IEEE Photonics Technology Letters* 24 (2012), pp. 61–63.